doublet exhibit *unusually large line widths*. This increased line width reflects either a slower rate of spin-state interconversion in FeP·CH_2Cl_2 compared to FeP or the fact that at any given temperature a sample of FeP·CH_2Cl_2 has a greater percentage of high-spin complexes than does FeP. The desolvation process of eliminating CH_2Cl_2 by mild heating of FeP·CH_2Cl_2 under vacuum does *not* seem to perturb the spin-crossover behavior of FeP; the same observables are found for a desolvated complex as for a microcrystalline sample of FeP prepared in such a way as to not incorporate a solvent molecule.

In this paper the nature of the spin-crossover complexes that give the "shoulders and bumps" seen in the Mössbauer spectra for ground samples of FeP, and for that matter the unperturbed microcrystalline FeP samples (**X** samples in previous paper), was examined. In the case of one pulverized sample the magnetic Mössbauer technique did indicate that the complexes giving the "bumps" in the *5 K zero-field spectrum* are due to high-spin ferric complexes. At this time there is no evidence either for or against the presence of FeP complexes interconverting at an intermediate rate.

In the previous paper no obvious intrinsic (i.e., isolated molecule) factors could be found to explain why FeP flips spin rapidly in the solid state compared to many N_4O_2 ferric complexes. In this paper data for "perturbed" samples of FeP have been presented to show that cooperative solid-state effects may influence the rate of spin-state interconversion. It appears that the low-temperature plateauing phenomenon, found for both "perturbed" compounds and for microcrystalline samples of various spin-crossover complexes, is a manifestation of slow kinetics for the high-spin $\rightleftharpoons$ low-spin transformation. Such behavior is also consistent with a mechanism of nucleation and growth. For all practical purposes the rate of "embryo formation" is equivalent to the spin-flipping rate.

Acknowledgment. We are grateful for support from NIH Grant HL 13652. Partial funding for the Mössbauer equipment came from NSF Grant CHE-78-20727, combined with equal funding from our Chemistry Department and the Research Board of the University of Illinois. We thank Mark Timken for running the 5 K Mössbauer spectra for sample **GD3**, both at zero field and with a 30-kG magnetic field.

Registry No. FeP, 79151-63-6; FeP·CH_2Cl_2, 92219-74-4.

Supplementary Material Available: EPR spectra for **D2** (Figure 6), ^{57}Fe Mössbauer spectra for **D1A** (Figure 7), and listings of microanalytical results (Table I), magnetic susceptibility data (Tables II and VI-VIII), interplanar spacings (Table III), and Mössbauer parameters (Table V) (13 pages). Ordering information is given on any current masthead page.

Contribution from the Department of Chemistry, The University of North Carolina, Chapel Hill, North Carolina 27514

An Electronic Structural Model for the Emitting MLCT Excited States of $Ru(bpy)_3^{2+}$ and $Os(bpy)_3^{2+}$

EDWARD M. KOBER* and THOMAS J. MEYER

Received May 1, 1984

A simple parametric model that includes spin–orbit coupling is developed for the localized MLCT excited states of $M(bpy)_3^{2+}$ (M = Ru, Os). In agreement with experimental data, it is found that there are three closely spaced (<200 cm^{-1}) low-lying states with a fourth state occurring several hundred cm^{-1} to higher energy. As has also been observed, it is predicted that emission from the lowest state is dipole forbidden. Complete state assignments are proposed on the basis of limited polarization data. In general, it is found that, for any Ru or Os bpy complex, no more than four low-lying MLCT states should be present.

Introduction

As a result of extensive applications of the excited states of $Ru(bpy)_3^{2+}$ (bpy = 2,2′-bipyridine) and related complexes as photocatalysts,[1] considerable effort has been expended in attempts to understand the electronic structure of these molecules and particularly of $Ru(bpy)_3^{2+}$ and $Os(bpy)_3^{2+}$.[2-18] The long-term goal of such work is the delineation of those features that control the various excited-state properties.

The relatively long-lived, luminescent excited states of $Ru(bpy)_3^{2+}$ and $Os(bpy)_3^{2+}$ are metal to ligand charge transfer (MLCT) in character,[2] and despite earlier assertions to the contrary,[3] it appears that they can be further characterized as being predominantly triplet states containing an appreciable amount of singlet character as a consequence of spin–orbit coupling.[4,5] The excited-state lifetimes of both complexes are temperature dependent and increase rather dramatically as the temperature is decreased.[6-11] This behavior has been successfully interpreted in terms of a thermally equilibrated Boltzmann population of several low-lying excited states whose lifetimes are temperature independent. Recent measurements

* To whom correspondence should be addressed at the Department of Chemistry, University of Arizona, Tucson, AZ 85721.

(1) (a) Meyer, T. J. *Acc. Chem. Res.* **1978**, *11*, 94–100. (b) Balzani, V.; Bolletta, F.; Gandolfi, M. T.; Maestri, M. *Top. Curr. Chem.* **1978**, *75*, 1–64. (c) Whitten, D. G. *Acc. Chem. Res.* **1980**, *13*, 83–90. (d) Sutin, N.; Creutz, C. *Adv. Chem. Ser.* **1978**, *No. 168*, 1–27. (e) Humphry-Baker, R.; Lilie, J.; Grätzel, M. *J. Am. Chem. Soc.* **1982**, *104*, 422–5. (f) Kalyanasundaram, K. *Coord. Chem. Rev.* **1982**, 46, 159–244.
(2) (a) Klassen, D. M.; Crosby, G. A. *J. Chem. Phys.* **1968**, *48*, 1853–8. (b) Zuloaga, F.; Kasha, M. *Photochem. Photobiol.* **1968**, *7*, 549–55.
(3) (a) Hipps, K. W.; Crosby, G. A. *J. Am. Chem. Soc.* **1975**, *97*, 7042–8. (b) Pankuch, B. J.; Lacky, D. E.; Crosby, G. A. *J. Phys. Chem.* **1980**, *84*, 2061–7.
(4) (a) Felix, F.; Ferguson, J.; Güdel, H. U.; Ludi, A. *Chem. Phys. Lett.* **1979**, *62*, 153–7. (b) Felix, F.; Ferguson, J.; Güdel, H. U.; Ludi, A. *J. Am. Chem. Soc.* **1980**, *102*, 4096–102. (c) Decurtins, S.; Felix, F.; Ferguson, J.; Güdel, H. U.; Ludi, A. *Ibid.* **1980**, *102*, 4102–6.
(5) Kober, E. M.; Meyer, T. J. *Inorg. Chem.* **1982**, *21*, 3967–77.
(6) (a) Hager, G. D.; Crosby, G. A. *J. Am. Chem. Soc.* **1975**, *97*, 7031–7. (b) Hager, G. D.; Watts, R. J.; Crosby, G. A. *Ibid.* **1975**, *97*, 7037–42.
(7) (a) Van Houten, J.; Watts, R. J. *Inorg. Chem.* **1978**, *17*, 3381–5. (b) Van Houten, J.; Watts, R. J. *J. Am. Chem. Soc.* **1976**, *98*, 4853–8.
(8) Allsopp, S. R.; Cox, A.; Kemp, T. J.; Reed, W. J. *J. Chem. Soc., Faraday Trans. 1* **1978**, *74*, 1275–89.
(9) Lacky, D. E.; Pankuch, B. J.; Crosby, G. A. *J. Phys. Chem.* **1980**, *84*, 2068–74.

0020-1669/84/1323-3877$01.50/0

suggest that thermal equilibrium may not be maintained at extremely low temperatures (<6 K), though.[12]

A precise description of the emitting states is a matter of current debate. For $Ru(bpy)_3^{2+}$, three relatively long-lived ($\tau \approx 10^{-6}$ s) MLCT states are required to explain the temperature-dependent lifetime behavior below 77 K.[6] At higher temperatures, an additional, nonspectroscopically observable state reveals its presence by temperature-dependent lifetime measurements. Since population of this state gives rise to photosubstitution, it has been assigned as a d–d state[7,8,13] and will be of no further concern here. For $Os(bpy)_3^{2+}$, three MLCT states are also required to explain the temperature-dependent lifetime behavior below 77 K.[9] Again, data for higher temperatures implies the presence of an additional state.[10] However, the relatively long lifetime of the state ($\tau \approx 10^{-8}$ s) and the absence of photosubstitution strongly suggest that the additional state is also an MLCT state and not a d–d state as appears to be the case for $Ru(bpy)_3^{2+}$. For Os, which is a third-row transition metal, the d–d states are expected to occur at $\geq 30\,000$ cm^{-1} and the energies of the states being discussed here are at 20 000 cm^{-1}. From the data for the osmium complex it thus appears that four low-lying MLCT states need to be accounted for on the basis of the experimental data, whereas previous theoretical studies have concentrated on explaining the presence of three low-lying excited states.[3,6,9,11]

The most important question that must be answered before a proper analysis of these states can be undertaken is "Are the excited states localized or delocalized?" That is, is the promoted electron localized in the π^* orbital of a single bpy ligand or is it delocalized over all three bpy ligands? The point has been discussed and debated extensively, with the accumulating evidence pointing quite clearly toward the localized alternative. The two most direct pieces of evidence are as follows: (1) The resonance Raman spectra of the excited states are clearly consistent with the presence of one reduced and two normal bpy ligands.[14] (2) Shifts in absorption spectra as a function of solvent are quantitatively consistent with an instantaneous sensing of the formation of the dipolar excited state $(bpy)_2M^{III}(bpy^{-\cdot})^{2+}$.[15]

It has also been pointed out that luminescence polarization ratio data are inconsistent with a high-symmetry (D_3) excited state but can be successfully modeled with a localized excited state.[16] Indirect evidence also exists in support of localization in that both EPR and absorption spectral measurements show that when an electron is added to the ground state to give $Ru(bpy)_3^+$, the added electron is localized on a single bpy ligand.[17,18] Overall, it seems very difficult to dispute the conclusion that the excited states are localized.

The ultimate test of the localized hypothesis is to develop an electronic structural model which would result in explicit state assignments that are consistent with the various experimental data. Previously, we have developed a parametric model for the absorption spectra of the ions $M(bpy)_3^{2+}$ (M = Fe, Ru, Os) based on the delocalized excited states *as required by exciton theory*.[5] The primary features of that analysis were to show how spin–orbit coupling at the metal affected the mixing between pure singlet and triplet states and how the degeneracy of the triplet states was lifted. Here, a similar parametric model for the localized excited states is developed, which leads to the prediction of certain properties for the low-lying excited states. Explicit assignments of the experimentally observed states are then attempted.

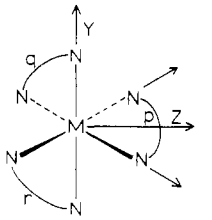

Figure 1. Coordinate system for the localized model with the promoted electron located on bpy p. The Z axis is the C_2 axis of bpy p, and the X axis is normal to the page.

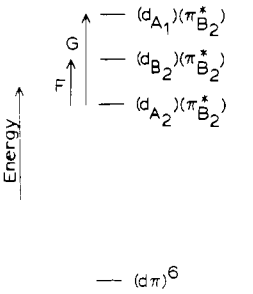

Figure 2. Relative energies of the $(d\pi)^5(\pi^*_{B_2})^1$ excited states and the $(d\pi)^6$ ground state. F and G are positive as shown.

Description of the Model

The development of the model proceeds in three discrete steps: (1) The excited-state configurations resulting from an electron residing in a bpy π^* orbital interacting with the d^5 metal core are presented. (2) The resulting configurations are resolved into pure singlet and triplet states by the introduction of spin–spin coupling. (3) The effect of the spin–orbit coupling due to the presence of the metal ion is calculated. The result is an electronic structural model that depends upon four parameters. An estimation of the parameters is then made to provide a prediction of the symmetry and relative energies of the various excited states.

The coordinate system used in the analysis is shown in Figure 1. The promoted electron is taken as residing in the π^* orbital of bpy ligand p, and the resulting molecule has C_2 symmetry. The C_2 axis of bpy p is taken as the Z axis, and the Y axis is selected as being perpendicular to the M–bpy p plane. If just the metal and unique bpy ligand were considered, the appropriate point group would be C_{2v}, and C_{2v} group symmetry labels will be used in describing the orbitals of the groups. The C_{2v} labels provide a convenient numbering scheme, and the electronic distortion from actual C_{2v} symmetry is probably not great. The C_2 symmetry labels are obtained by merely dropping the numerical subscript.

The symmetries of the various orbitals are readily defined. The lowest energy π^* orbital of bpy is known to have B_2 symmetry (where the plane of the molecule is the XZ plane).[19] This orbital is symmetrical with regard to reflection through the YZ plane. The next lowest π^* orbital has A_2 symmetry and occurs ~7000 cm^{-1} higher in energy. In- and out-of-phase

(10) Allsopp, S. R.; Cox, A.; Kemp, T. J.; Reed, W. J.; Carassiti, V.; Traverso, O. *J. Chem. Soc., Faraday Trans. 1* **1979**, *75*, 353–62.
(11) Harrigan, R. W.; Crosby, G. A. *J. Chem. Phys.* **1973**, *59*, 3468–76.
(12) Ferguson, J.; Krausz, E. R. *Chem. Phys. Lett.* **1982**, *93*, 21–5.
(13) Durham, B.; Caspar, J. V.; Nagle, J. K.; Meyer, T. J. *J. Am. Chem. Soc.* **1982**, *104*, 4803–10.
(14) (a) Bradley, P. G.; Kress, N.; Hornberger, B. A.; Dallinger, R. F.; Woodruff, W. H. *J. Am. Chem. Soc.* **1981**, *103*, 7441–6. (b) Dallinger, R. F.; Woodruff, W. H. *Ibid.* **1979**, *101*, 4391–3.
(15) Kober, E. M.; Sullivan, B. P.; Meyer, T. J. *Inorg. Chem.* **1984**, *23*, 2098–104.
(16) (a) Carlin, C. M.; DeArmond, M. K. *Chem. Phys. Lett.* **1982**, *89*, 297–302. DeArmond, M. K.; Carlin, C. M.; Huang, W. L. *Inorg. Chem.* **1980**, *19*, 62–7. (c) Hipps, K. W. *Ibid.* **1980**, *19*, 1390–2.
(17) Motten, A. G.; Hanck, K.; DeArmond, M. K. *Chem. Phys. Lett.* **1981**, *79*, 541–6.
(18) Heath, G. A.; Yellowlees, L. J.; Braterman, P. S. *Chem. Phys. Lett.* **1982**, *92*, 646–8.
(19) König, E.; Kremer, S. *Chem. Phys. Lett.* **1970**, *5*, 87–90.

Table I. Relative Excited-State Energies from the Localized Model prior to Spin-Orbit Coupling

orbital composition	sym label	energy
$(d_{B_2})(\pi^*_{B_2})$	$^1A_1$: $1A_1$	$F+K$
	$^3A_1$: $1A_2, 1B_1, 1B_2$	$F-K$
$(d_{A_2})(\pi^*_{B_2})$	$^1B_1$: $2B_1$	$+K$
	$^3B_1$: $2A_1, 2A_2, 2B_2$	$-K$
$(d_{A_1})(\pi^*_{B_2})$	$^1B_2$: $3B_2$	$G+K$
	$^3B_2$: $3A_1, 3A_2, 3B_1$	$G-K$

combinations of the B_2 π^* orbitals of the two nonreduced bpy ligands (q and r) give rise to MO's of A and B symmetry, respectively. In C_{2v} symmetry, the three $d\pi$ (t_{2g}) orbitals transform as A_1, A_2, and B_2. The $d\pi$ orbitals are defined in terms of the symmetry axes and in terms of angular momentum functions in eq 1. There are five metal valence

$$d\pi_{A_1} = d_{Z^2-X^2} = |20\rangle(3/4)^{1/2} - (|22\rangle + |2{-2}\rangle)/2$$
$$d\pi_{A_2} = d_{XY} = (|22\rangle - |2{-2}\rangle)/2^{1/2} \quad (1)$$
$$d\pi_{B_2} = d_{YZ} = (|21\rangle + |2{-1}\rangle)/2^{1/2}$$

electrons to be placed in the three $d\pi$ orbitals in the MLCT excited states, and three different $(d\pi)^5(\pi^*_{B_2})^1$ excited-state configurations can result depending upon which $d\pi$ orbital is only singly occupied. For brevity, the $(d\pi)^5$ core states are designated by indicating which orbital contains the "hole" and dropping the "π" label, i.e., $d_{A_1} = (d\pi_{A_1})^1(d\pi_{A_2})^2(d\pi_{B_2})^2$. The relative energies of the configurations can be described by two parameters, which are labeled F and G. Arbitrarily selecting the $(d_{A_2})(\pi^*_{B_2})$ configuration as the reference point, the $(d_{B_2})(\pi^*_{B_2})$ configuration is set as occurring at energy F, and $(d_{A_1})(\pi^*_{B_2})$ at energy G. The $(d_{A_2})(\pi^*_{B_2})$ configuration occurs at lowest energy if F and G are both positive. The situation with $0 < F < G$ is illustrated in Figure 2.

Next, the coupling of the spin on the promoted electron to the spin on the odd electron in the d^5 core is introduced. The spin–spin coupling resolves each of the excited-state configurations into singlet and triplet states. Although the splitting between singlet and triplet states should be different for each of the three configurations, they will be approximated as being equal since we are interested in keeping the model as simple as possible and do not know of a reliable method for obtaining more exact values. In all three cases an electron in a bpy π^* orbital is being coupled to an electron in a metal $d\pi$ orbital, so that the approximation may not be too drastic. As a result, in the model it is assumed that all of the singlet states are destabilized by an amount K and the triplet states are stabilized by the same amount K. K is the exchange integral between $\pi^*_{B_2}$ and the singly occupied $d\pi$ orbital.[20]

The relative energies of the pure singlet and triplet excited states are presented in Table I in terms of the parameters F, G, and K. The states are listed first by their parent configuration, then by their spin and spatial symmetry labels, and finally by their total symmetry labels. The total symmetry is the product of the spin and spatial symmetries. In the C_{2v} point group, the singlet spin function $|\alpha\beta\rangle - |\beta\alpha\rangle$ transforms as A_1, and the triplet spin functions $|\alpha\beta\rangle + |\beta\alpha\rangle$, $|\alpha\alpha\rangle + |\beta\beta\rangle$, and $|\alpha\alpha\rangle - |\beta\beta\rangle$ transform as A_2, B_1, and B_2, respectively. The numbers preceding the total symmetry labels are an arbitrary numbering scheme used to distinguish the various states. The explicit antisymmetrized wave functions are listed in Table II. Note from these results that the degeneracy of the triplet states is completely removed so that each gives rise to three distinct states.

The final step in the development of the model is to include the effects of spin–orbit coupling due to the presence of the transition metal. Two standard approximations are made in incorporating these effects:[5,21] (1) The extent of mixing between metal and ligand orbitals is assumed to be small. (2) The mixing of the metal and ligand orbitals is assumed to be isotropic. With the approximations in mind, the spin–orbit coupling matrix elements between the excited states can be reduced to the matrix elements between the various d^5 configurations of the metal, viz., $\langle (d_n)(\pi^*_{B_2})|H_{SO}|(d_{n'})(\pi^*_{B_2}{}')\rangle = \langle d_n|H_{SO}|d_{n'}\rangle\langle \pi^*_{B_2}|\pi^*_{B_2}{}'\rangle$, where the spin of the electron is included as part of the wave functions. Here, d_n represents the d^5 wave function and H_{SO} is the spin–orbit coupling operator, which has the form $H_{SO} = \lambda(L_ZS_Z + (L_+S_- + L_-S_+)/2)$. The term λ is the spin–orbit coupling constant, taken to be the same for all configurations, and L and S are the angular and spin momentum operators, respectively.

The matrix elements between the d^5 configurations are readily calculated by using the wave functions given in eq 1. The results are given in eq 2. Since the complete five-electron

$$\begin{array}{c} |d_{A_1}\alpha\rangle \\ (|d_{A_1}\beta\rangle) \end{array} \quad \begin{array}{c} |d_{A_2}\alpha\rangle \\ (|d_{A_2}\beta\rangle) \end{array} \quad \begin{array}{c} |d_{B_2}\beta\rangle \\ (|d_{B_2}\alpha\rangle) \end{array}$$
$$\begin{bmatrix} 0 & -\lambda/2 & -\lambda/2 \\ -\lambda/2 & 0 & -\lambda/2 \\ -\lambda/2 & -\lambda/2 & 0 \end{bmatrix} \quad (2)$$

wave functions are used to calculate the matrix, rather than the "hole" formalism, λ is intrinsically positive. With the use of the matrix in conjunction with the complete antisymme-

Table II. Explicit Wave Functions from the Localized Excited-State Model prior to Spin-Orbit Coupling

states	wave functions
$1A_1$	$^1/_2(d_{B_2}\pi^*_{B_2} + \pi^*_{B_2}d_{B_2})(|\alpha\beta\rangle - |\beta\alpha\rangle)$
$2A_1$	$^1/_2(d_{A_2}\pi^*_{B_2} - \pi^*_{B_2}d_{A_2})(|\alpha\alpha\rangle + |\beta\beta\rangle)$
$3A_1$	$^1/_2(d_{A_1}\pi^*_{B_2} - \pi^*_{B_2}d_{A_1})(|\alpha\alpha\rangle - |\beta\beta\rangle)$
$1A_2$	$^1/_2(d_{B_2}\pi^*_{B_2} - \pi^*_{B_2}d_{B_2})(|\alpha\beta\rangle + |\beta\alpha\rangle)$
$2A_2$	$^1/_2(d_{A_2}\pi^*_{B_2} - \pi^*_{B_2}d_{A_2})(|\alpha\alpha\rangle - |\beta\beta\rangle)$
$3A_2$	$^1/_2(d_{A_1}\pi^*_{B_2} - \pi^*_{B_2}d_{A_1})(|\alpha\alpha\rangle + |\beta\beta\rangle)$
$1B_1$	$^1/_2(d_{B_2}\pi^*_{B_2} - \pi^*_{B_2}d_{B_2})(|\alpha\alpha\rangle + |\beta\beta\rangle)$
$2B_1$	$^1/_2(d_{A_2}\pi^*_{B_2} + \pi^*_{B_2}d_{A_2})(|\alpha\beta\rangle - |\beta\alpha\rangle)$
$3B_1$	$^1/_2(d_{A_1}\pi^*_{B_2} - \pi^*_{B_2}d_{A_1})(|\alpha\beta\rangle + |\beta\alpha\rangle)$
$1B_2$	$^1/_2(d_{B_2}\pi^*_{B_2} - \pi^*_{B_2}d_{B_2})(|\alpha\alpha\rangle - |\beta\beta\rangle)$
$2B_2$	$^1/_2(d_{A_2}\pi^*_{B_2} - \pi^*_{B_2}d_{A_2})(|\alpha\beta\rangle + |\beta\alpha\rangle)$
$3B_2$	$^1/_2(d_{A_1}\pi^*_{B_2} + \pi^*_{B_2}d_{A_1})(|\alpha\beta\rangle - |\beta\alpha\rangle)$

Table III. Spin–Orbit Coupling Matrices for the Localized Excited-State Model

Matrix I

$1A_1$	$2A_1$	$3A_1$
$F+K$	$-\lambda/2$	$-\lambda/2$
$-\lambda/2$	$-K$	$-\lambda/2$
$-\lambda/2$	$-\lambda/2$	$G-K$

Matrix II

$1A_2$	$2A_2$	$3A_2$
$F-K$	$-\lambda/2$	$-\lambda/2$
$-\lambda/2$	$-K$	$-\lambda/2$
$-\lambda/2$	$-\lambda/2$	$G-K$

Matrix III

$1B_1$	$2B_1$	$3B_1$
$F-K$	$-\lambda/2$	$-\lambda/2$
$-\lambda/2$	K	$-\lambda/2$
$-\lambda/2$	$-\lambda/2$	$G-K$

Matrix IV

$1B_2$	$2B_2$	$3B_2$
$F-K$	$-\lambda/2$	$-\lambda/2$
$-\lambda/2$	$-K$	$-\lambda/2$
$-\lambda/2$	$-\lambda/2$	$G+K$

(20) Levine, I. N. "Quantum Chemistry", 2nd ed.; Allyn and Bacon: Boston, 1974; p 205.

(21) Piepho, S. B.; Schatz, P. N.; McCaffery, A. J. *J. Am. Chem. Soc.* **1969**, *91*, 5994–6001.

trized wavefunctions given in Table II, the spin–orbit coupling matrix elements between the excited states are readily calculated. The results of the calculations, including the zero-order energies from Table I along the diagonals, are given in Table III. The eigenvalues and eigenvectors of these matrices then give the relative energies and compositions, respectively, of the excited states in terms of the pure triplet and singlet states of Tables I and II.

Several general features of the model deserve emphasis at this point. It is seen that each configuration gives rise to four states, each of a different symmetry type. Thus, the triplet states of a particular configuration cannot mix with the singlet state from the same configuration, but only with singlet states from other configurations. There are only three singlet states, and they have A_1, B_1, and B_2 symmetries. It follows that all of the triplet states that have one of these three symmetry types have a singlet state available to mix with and could thus acquire some singlet character. There is not, however, a singlet state of A_2 symmetry, and A_2 states must remain pure triplet states, although they do so only at the present level of approximation. For example, some of the higher lying π^* orbitals of bpy have A_2 symmetry, so that the singlet components of the $(d_{A_1})(\pi^*_{A_2})$ configurations do have A_2 symmetry. Mechanisms probably exist by which these states could mix with the triplet A_2 states to provide the latter with some singlet character. Also, because of the lack of rigorous C_{2v} symmetry, there could be mixing between the A_2 and A_1 states. However, we presume that such effects are relatively small compared to the mixing provided by direct spin–orbit coupling. The A_2 states are therefore treated here as essentially pure triplet states.

Analysis

With the details of a parametric model for the excited states now available, it should be possible to make predictions concerning various excited-state properties. In order to proceed, it is first necessary to make estimates of the values of the various parameters. The value of the exercise is that it provides approximate values for the relative energies and compositions of the states, which in turn can be used to predict various physical properties. One of the primary properties of concern is the polarization of emitted light for the various states.

Values for two of the parameters, K and λ, can be arrived at in a direct manner. Spin–orbit coupling constants for the free M^{3+} ions are reasonably well-known: λ_{Ru} = 1180–1250 cm^{-1}; λ_{Os} = 3000–3500 cm^{-1}.[22] Experimentally derived values for M(III) complexes are also known: λ_{Ru} = 880–1100 cm^{-1};[23,24] λ_{Os} = 2600–3000 cm^{-1}.[24,25] In line with these values, our earlier analysis of the absorption spectra of the complexes $M(bpy)_3^{2+}$ gave λ_{Ru} = 1200 cm^{-1} and λ_{Os} = 3000 cm^{-1}. The same analysis gave K = 850 cm^{-1} for both metals, which appeared to be reasonable compared to the results of related analyses for very different metal complexes. The values of λ and K derived from the analysis of the absorption spectra will be used in the present analysis.

Unfortunately, we know of no reliable method to predict the values of F and G, and they must be treated as variables. From analyses of the near-infrared absorption spectra of Os(III) complexes it has been found that ligand field contributions can split the $d\pi$ orbitals by up to several thousand

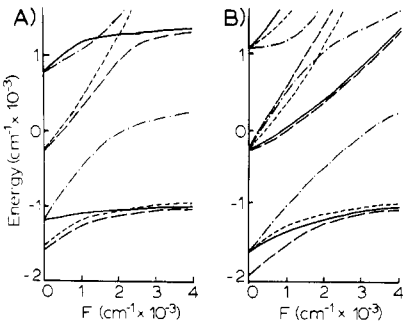

Figure 3. Relative energies of the lower lying MLCT excited states of $Ru(bpy)_3^{2+}$. State symmetries are indicated as follows: (---) A_1; (–·–·) B_1; (– –) A_2; (—) B_2. (A) λ = 1200 cm^{-1}, K = 850 cm^{-1}, and G = 2000 cm^{-1}. (B) λ = 1200 cm^{-1}, K = 850 cm^{-1}, and $2G = F$.

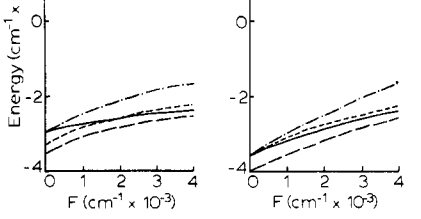

Figure 4. Relative energies of the lower lying MLCT excited states of $Os(bpy)^{2+}$. State symmetries are indicated as follows: (---) A_1; (–·–·) B_1; (– –) A_2; (—) B_2. (A) λ = 3000 cm^{-1}, K = 850 cm^{-1}, and G = 2000 cm^{-1}. (B) λ = 3000 cm^{-1}, K = 850 cm^{-1}, and $2G = F$.

cm^{-1}.[26] Consequently, the relative energies of the states as a function of F and G were examined over the range $0 < |F,G| < 4000$ cm^{-1}.

Examples of such variations are shown in Figure 3 for Ru and in Figure 4 for Os. (Note the different energy scales.) In part A, in both cases, G was set equal to 2000 cm^{-1} while F was varied over the range 0–4000 cm^{-1}. In part B, F was also varied from 0 to 4000 cm^{-1} while the relationship $F = 2G$ was maintained. Because of the similarities between the matrices in Table III, similar plots will be obtained for negative values of F and/or G although the ordering of the states will change. However, the general features of the energy variations with F and G are illustrated by the present figures. As noted later, the available polarization data are consistent with the order $0 < F < G$.

The most important point to arise in the analysis is that there are four lowest lying states that remain fairly close in energy over a broad range of F and G values and that are separated from higher lying states by at least 800 cm^{-1} for Ru and at least 3000 cm^{-1} for Os. Assuming that the populations amongst the various states are maintained in a thermal equilibrium, at room temperature the population of the fifth lowest lying state will be less than 10^{-3} of the fourth state and less than 10^{-5} of the lowest state in the four-state manifold. Consequently, unless the upper states are extremely short-lived, their contributions to excited-state properties should be negligible at ambient or lower temperatures. We will thus neglect all states above the four-state manifold from further consideration. There is one nondegenerate state of each symmetry in the four-state manifold, and for simplicity we will designate each by its symmetry label. This point is important because, in a parametric delocalized model developed previously,[5] five

(22) (a) Goodman, B. A.; Raynor, J. B. *Adv. Inorg. Chem. Radiochem.* **1970**, *13*, 192. (b) Figgis, B. N.; Lewis, J. *Prog. Inorg. Chem.* **1964**, *6*, 99. (c) Dunn, T. M. *Trans. Faraday Soc.* **1961**, *57*, 1441–4.
(23) (a) Figgis, B. N.; Lewis, J.; Mabbs, F. E.; Webb, G. A. *J. Chem. Soc. A* **1966**, 422–6. (b) Figgis, B. N.; Lewis, J.; Nyholm, R. S.; Peacock, R. D. *Discuss. Faraday Soc.* **1958**, *26*, 103–9.
(24) Hudson, A.; Kennedy, M. J. *J. Chem. Soc. A* **1969**, 1116–20.
(25) Hill, N. J. *J. Chem. Soc., Faraday Trans. 2* **1972**, *68*, 427–34.
(26) (a) Kober, E. M. Ph.D. Dissertation, The University of North Carolina, Chapel Hill, NC, 1982. (b) Kober, E. M.; Meyer, T. J. *Inorg. Chem.* **1983**, *22*, 1614–6.

low-lying states were predicted, three of which had E symmetry. This should prove to be the key feature in establishing which model is correct.

The appearance of four lowest lying states is a consequence of the pseudo-C_{2v} symmetry of the molecules and the value of λ and is independent of the values of F, G, and K. The C_{2v} symmetry allows the $d\pi_{A_2}$ and $d\pi_{A_2}$ orbitals to be defined as orthogonal, which in turn results in the relatively simple matrices shown in Table III. The descent to C_2 symmetry by displacing the ligands from ideal octahedral positions causes $d\pi_{A_1}$ and $d\pi_{A_2}$ to mix, which leads to a mixing of the A_1 and A_2 states and of the B_1 and B_2 states. However, it seems doubtful that the $d\pi_{A_1}$–$d\pi_{A_2}$ interaction is significant since the N–M–N angles are close to 90° (80–100°).[27]

The form of the matrices, with all off-diagonal elements equal to $-\lambda/2$, determines that there will be no more than four lowest lying states. This form requires that the lowest lying state of a matrix be lower in energy than the second state by at least the amount λ. This case results if two of the diagonal elements are equal and the third is infinitely large. For finite values of all three diagonal elements, the separation must be greater than λ. For second- and third-row transition metals where $\lambda \geq 1000$ cm^{-1}, it is guaranteed that only the lowest state from each matrix need be considered at ambient or lower temperatures. Since there are only four matrices, one for each of the four symmetries, a maximum of four low-lying states results. Depending upon the values of F, G, and K, it may result that the four states are not closely spaced and that contributions from fewer than four states are needed to account for the excited-state behavior. This is a noteworthy result since the same basic model developed here should also apply to mono- and bis(bipyridine) complexes. Clearly, in such complexes, a different ordering of low-lying states could emerge than will be proposed here and the actual order will depend on the relative magnitudes of F, G, and K. However, no more than four low-lying states are expected.

The second important point to emerge from our relatively simple model concerns the character of the four lowest states. If F and G are both positive and large compared to λ, the three lowest states of the four states become almost degenerate in energy while the fourth state appears $\sim 2K$ higher in energy (see Figures 3 and 4). Projection back into the original basis states (Tables I and II) reveals that the composition of the uppermost state (B_1) is essentially all $^2B_1$, which is the singlet state of the $(d_{A_2})(\pi^*_{B_2})$ configuration. The remaining three states (A_1, A_2, B_2) are found to correspond to the triplet states ($^2A_2$, $^2B_1$, $^2B_2$) of the same configuration.

As F and G are made smaller, but still positive, appreciable character from states of the other two configurations are mixed in. However, the A_1, A_2, and B_2 states all remain predominantly $(d_{A_2})(\pi^*_{B_2})$ in character. The $^1B_1$ state remains predominantly $(d_{A_2})(\pi^*_{B_2})$ in character only until F or G becomes smaller than $2K$. At that point, the zero-order energy of the triplet component of one of the higher energy configurations becomes lower than the zero-order energy of $^2B_1$, which is the singlet component of the $(d_{A_2})(\pi^*_{B_2})$ state. This triplet state would then become the predominant contributor to the B_1 state. It can be shown that, in general, the three lowest energy states in the four-state manifold will be predominantly composed of triplet constituents of the lowest energy configuration. The fourth state could be composed predominantly either of the singlet constituent of this configuration or of a triplet constituent of the second lowest configuration.

The question of the relative amounts of singlet and triplet character in the emitting excited states of these complexes has long been debated.[3-5] From our model, quantitative estimates

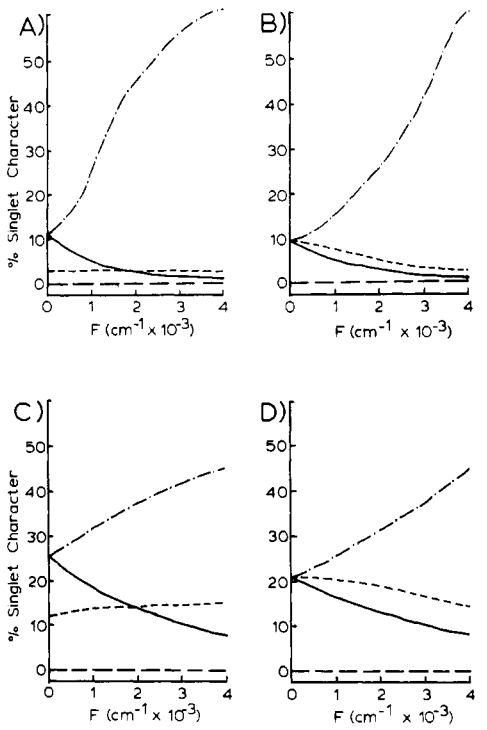

Figure 5. Percent singlet character in the four lowest lying MLCT excited states of $Ru(bpy)_3^{2+}$ (A, B) and $Os(bpy)_3^{2+}$ (C, D). State symmetries are indicated as follows: (- - -) A_1; (- · - ·) B_1; (– –) A_2; (—) B_2. (A) $\lambda = 1200$ cm^{-1}, $K = 850$ cm^{-1}, and $G = 2000$ cm^{-1}. (B) $\lambda = 1200$ cm^{-1}, $K = 850$ cm^{-1}, and $2G = F$. (C) $\lambda = 3000$ cm^{-1}, $K = 850$ cm^{-1}, and $G = 2000$ cm^{-1}. (D) $\lambda = 3000$ cm^{-1}, $K = 850$ cm^{-1}, and $2G = F$.

for the spin compositions of the four lowest states can easily be made and the results are illustrated in Figure 5. In Figure 5 is plotted the percent singlet character of the four lowest states as a function of F and G with use of the same range of values as in Figures 3 and 4. The plots show that the three lowest states (A_1, A_2 B_2) have relatively little singlet character, whereas the singlet contribution to the higher B_1 state varies strongly with G and F. For Ru, the lowest three states are found to have less than 11% singlet character, and for Os, the limit is 26%. This conclusion depends only upon K and λ and applies for all values of F and G. For large values of F and G, the three lowest states are found to have very little singlet character ($\sim$5% for Ru and $\sim$15% for Os), while the fourth state (B_1) becomes predominantly singlet in nature. Overall, it seems appropriate to describe the three lowest states as "triplet" states although the fourth state evades such a characterization. It is of particular interest that the "triplet" states of Os have 2–5 times as much singlet character as the Ru analogues. A similar conclusion had been reached earlier from an analysis of the absorption spectra.[5]

The third important point of the model concerns the relative energies of the four states. These are also found to vary in a general way with the parameters F and G. The main feature here is that the A_2 state is always lowest lying regardless of the values of F, G, K, or λ. This is a consequence of the fact that the A_2 state is a mixture of a triplet component from each of the three configurations whereas the other three states are mixtures of two triplets and one singlet state. The average energy of the contributors to the A_2 state must then be lower than for any other state, and since the matrices are identical in all other respects, this requires that the lowest A_2 state must be the lowest energy state.

The ordering of the remaining three states depends upon the values of F and G. As mentioned above, the highest energy of the four states is of the same symmetry as the singlet state

(27) Rillema, D. P.; Jones, D. S.; Levy, H. A. *J. Chem. Soc., Chem. Commun.* **1979**, 849–51.

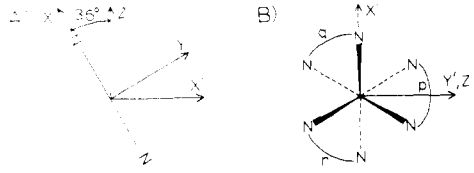

Figure 6. Relationship between the coordinates of the localized model (X, Y, Z) and those of the D_3 molecule (X', Y', Z'): (A) view down the $Z(Y')$ axis; (B) view down the Z' axis. X' is in the plane of the page.

of the lowest lying configuration. For the case illustrated here with $0 < F, G$ the symmetry is B_1. The second highest lying of the four states will have the same symmetry as the singlet state of the second lowest lying configuration. For the order $0 < F < G$ the symmetry is B_2, and for the order $0 < G < F$ the symmetry is A_1. The symmetry of the second lowest lying of the four states is the same as that of the singlet state of the highest lying of the three configurations. For the order $0 < F < G$, this would be A_1, and for the order $0 < G < F$, it would be B_2. These relationships are, of course, based on the assumption that all three configurations have the same K value.

Excited-State Properties. The excited-state property that can be most directly predicted by our model is that of the polarization of emission. A complication in this regard is that the axes for the localized model must be related to the D_3 symmetry coordinates since these constitute the frame of reference for the molecule. The relationship between the two is shown in Figure 6, where the D_3 symmetry axes are labeled with primes to distinguish them from the axes adopted to establish the localized model. The Z' axis is collinear with the molecular C_3 axis and is perpendicular to the Z axis. The Z axis constitutes the C_2 axis of a bipyridine ligand. Since the X' and Y' axes are equivalent by symmetry, the Y' axis is arbitrarily taken to be collinear with the Z axis. From the crystal structure of $[Ru(bpy)_3](PF_6)_2$, the angle between the X and Z' axes is found to be 36°.[27]

Because of the presence of the molecular C_3 axis, it is only possible to define an experimentally observable light polarization as being either Z' or X',Y'. The predictions concerning emission polarization from the various states based on dipole selection rules are then readily found to be as follows: (1) A_1, $Z = X',Y'$; (2) B_1, $X = 0.65Z' + 0.35X',Y'$; (3) B_2, $Y = 0.35Z' + 0.65X',Y'$; (4) A_2, dipole forbidden. It is interesting to note that, because of the canting of the localized model axes relative to the D_3 symmetry axes, the emission from the B_1 and B_2 (and possibly A_2) states should show up in both Z' and X',Y' polarizations. This situation is in sharp contrast to the predictions of the symmetric, delocalized model, where emission from any one state should be Z' or X',Y' polarized, but not both.[3,4]

It is also possible to predict directly the polarization ratio (P) of emission for randomly oriented molecules. This ratio is defined as $P = (I_\parallel - I_\perp)/(I_\parallel + I_\perp)$, where $I_\parallel$ and $I_\perp$ are the intensities of the components of the luminescence that are polarized parallel and perpendicular, respectively, to the polarization of the exciting light.[28] Defining θ as the angle between the absorption and emission oscillators, the value of P can then be expressed as in eq 3, where $\langle\cos^2\theta\rangle$ is the

$$P = \frac{2\langle\cos^2\theta\rangle - 1}{\langle\cos^2\theta\rangle + 3} \qquad (3)$$

average value of $\cos^2\theta$. Absorption spectra for the $M(bpy)_3^{2+}$ ions were found to be generally consistent with there being only two types of absorption oscillators: one planar and X',Y' polarized, and one linear and Z' polarized.[4] The expected values of P for these two cases for the various excited states are listed in Table IV.

Table IV. Properties of the Four Lowest Lying Excited States for $M(bpy)_3^{2+}$

state	emission polarizn	$P(X',Y')^a$	$P(Z')^b$
A_1	$Z = X',Y'$	0.14	−0.33
B_1	$X = 0.65Z' + 0.35X',Y'$	−0.15	0.26
B_2	$Y = 0.35Z' + 0.65X',Y'$	−0.01	0.01
A_2	dipole forbidden		

[a] Value of P if absorption is X',Y' polarized. [b] Value of P if absorption is Z' polarized.

Table V. Excited-State Properties of $Os(bpy)_3^{2+}$ [a]

state	energy, cm^{-1}	k_{nr}, s^{-1}	k_r, s^{-1}	ϕ_{em}
4	607	1.9×10^8	$(9.6 \times 10^5)^b$	$(0.005)^b$
3	52	3.0×10^6	1.2×10^5	0.038
2	16	1.9×10^5	8.2×10^3	0.041
1	0	8.8×10^4	3.0×10^3	0.033

[a] From ref 9 and 10. [b] See text.

Table VI. Excited-State Properties of $Ru(bpy)_3^{2+}$ [a]

state	energy, cm^{-1}	k_{nr}, s^{-1}	k_r, s^{-1}	ϕ_{em}
3	61.2	1.0×10^6	5.9×10^5	0.404
2	10.1	4.1×10^4	1.2×10^4	0.230
1	0	4.8×10^3	9.2×10^2	0.167

[a] From ref 6.

Assignments. With the properties of the localized model in hand, it is possible to examine the available experimental data with the goal of making definitive state assignments or of uncovering possible disagreements. A first consideration is the number of MLCT states and their relative energies. The necessary information is obtainable from the temperature dependence of excited-state lifetimes and emission quantum yields with the assumption that the populations of the states involved are dictated by Boltzmann statistics. Data and analyses of this kind have appeared for $Ru(bpy)_3^{2+}$ [6] and $Os(bpy)_3^{2+}$ [9] in poly(methylmethacrylate) matrices in the temperature range 1.7–77 K and for $Os(bpy)_3^{2+}$ in a cellulose acetate matrix in the temperature range 77–300 K.[10] The data that have been obtained are summarized in Tables V and VI for $Os(bpy)_3^{2+}$ and $Ru(bpy)_3^{2+}$, respectively.

In the tables, k_{nr} and k_r are the nonradiative and radiative decay rate constants, respectively, and ϕ_{em} is the quantum yield for emission. For $Os(bpy)_3^{2+}$, the lifetime of state 3 was obtained from both the low- and high-temperature studies and the values are in agrement within experimental error. The quantum yield of emission for state 4 of $Os(bpy)_3^{2+}$ has not been measured directly, and the value of $\phi_{em} = 0.005$ as measured for the complex in acetonitrile solution at room temperature[29] is assumed since state 4 should dominate excited-state properties at this temperature. Also, it should be noted that, in the original analyses of the low-temperature data, it was assumed that state 2 was doubly degenerate.[6,9] Since there are no degeneracies possible for localized excited states, in the model developed here the k_{nr} and k_r values for state 2 should be increased by a factor of 2.

A first point that emerges from the data is that no more than four low-lying MLCT states are needed to explain the temperature-dependent properties of the excited states, which is in agreement with the prediction of the present model. Secondly, although the three lowest lying states are quite close

(28) (a) Fujita, I.; Kobayashi, H. *Inorg. Chem.* **1973**, *12*, 2758–62. (b) Albrecht, A. C. *J. Mol. Spectrosc.* **1961**, *6*, 84–108.

(29) Caspar, J. V.; Kober, E. M.; Sullivan, B. P.; Meyer, T. J. *J. Am. Chem. Soc.* **1982**, *104*, 630–2.

together in energy and are within 100 cm^{-1}, the fourth state for $Os(bpy)_3^{2+}$ lies ~600 cm^{-1} to higher energy. Such an ordering is in agreement with the prediction of the present model when one of the three excited-state configurations is significantly lower in energy than the other two, which is the case illustrated in Figures 3 and 4 when F and G are both large.

The question then arises as to the possible existence of a fourth low-lying MLCT state for $Ru(bpy)_3^{2+}$. Previously, it had been assumed that the three lowest states for $Os(bpy)_3^{2+}$ correspond to the three lowest states for $Ru(bpy)_3^{2+}$ (i.e. Os(1) → Ru(1), Os(2) → Ru(2), Os(3) → Ru(3)).[9] The basis for the correspondence was the similarity in energy spacings for the two complexes. Recently, we have shown that relative values of k_{nr} and k_r for the corresponding states for the two complexes can be accounted for quantitatively by available theoretical equations for k_{nr} and k_r,[26a,30] which gives strong support to the proposed correspondence between states. The same ordering of the lowest three states and the similarity in energy spacings suggests similar electronic structures and, therefore, similar F and G values for the Os and Ru excited states. As a consequence, it seems reasonable to expect that the fourth MLCT state for $Ru(bpy)_3^{2+}$ may also lie several hundred cm^{-1} above the low-lying manifold which includes the lowest three states. This is the case illustrated in Figures 3 and 5 for large values of F and G.

Unfortunately, the ability to observe the fourth MLCT state for $Ru(bpy)_3^{2+}$ is probably masked by a surface-crossing process to give low-lying d–d states.[7,8,13,31] The surface-crossing process with $E_a \approx 3500$ cm^{-1} and a preexponential term of 10^{12}–10^{14} s^{-1}, depending on the solvent,[31a] completely dominates the excited-state lifetime properties over the range of temperatures where the proposed fourth MLCT state should appear. However, since the d–d state does not appear to luminesce appreciably, the fourth MLCT state might be detectable from changes in emission spectra as a function of temperature. Quite recently evidence for a fourth low-lying MLCT state has been obtained from the polarized emission spectra of single crystals of $[Ru(bpy)_3](PF_6)_2$.[32] The temperature-dependent (243–343 K) changes in the polarized emission spectrum suggested the presence of a fourth MLCT state at 640 cm^{-1} (±20%) above the lowest MLCT state. Further, it was found that emission from the fourth state is quite weak, which is consistent with the low value of ϕ_{em} surmised for state 4 of $Os(bpy)_3^{2+}$ as shown in Table V. Thus, as predicted by the present model, four low-lying MLCT states appear to exist for both $Os(bpy)_3^{2+}$ and $Ru(bpy)_3^{2+}$ and the correspondence in their relative energies can be accounted for.

The ultimate test for the model is in explicit state assignments, but such assignments require detailed temperature-dependent polarization data if they are to be made unambiguously. Unfortunately, the data for $Ru(bpy)_3^{2+}$ are somewhat incomplete and very little data have been reported for $Os(bpy)_3^{2+}$. A summary of the available data for $Ru(bpy)_3^{2+}$ is as follows: (1) State 3 dominates the emission spectrum from 25 to >343 K.[6,32] Over this temperature range, the emission is at least 75% X',Y' polarized,[16c] and the observed value of the polarization ratio for predominantly X',Y'-polarized absorption is found to be $P \approx 0.10$.[4,6,16,28a] (2) At 7 K, where state 2 should be the dominant emitting state,[6] the emission is also reported to be predominantly X',Y' polarized.[12] (3) The emission from state 4 appears to be predominantly Z' polarized.[32] For $Os(bpy)_3^{2+}$, the only report is that at 77 K, where state 3 should be the dominant emitting state,[9,10] the polarization ratio for predominantly X',Y' polarized absorption is $P \approx 0.12$.[16a]

Albeit somewhat limited, the data are sufficient to suggest a unique state assignment. Since the A_2 state is calculated to always be lowest lying regardless of the values of F and G, state 1 can be assigned as A_2. Additional evidence in support of this assignment is discussed below. That $P(X',Y')$ for state 3 is found to be in rough agreement with the value of $P(X',Y') = 0.14$ for the A_1 state (see Table IV) leads to the assignment of state 3 as A_1. By a process of elimination, the predominance of X',Y' polarization in the emission of state 2 implies that it should be assigned as B_2. The suggested predominance of Z'-polarized emission for state 4 is consistent with its assignment as B_1. Thus, the complete state assignment as 1 = A_2, 2 = B_2, 3 = A_1, and 4 = B_1 is arrived at and has preliminary support from the available polarization data.

There is additional support for the assignment of the state 1 as A_2. Experimentally, at temperatures where state 1 is the dominant emitting state for $Ru(bpy)_3^{2+}$, the emission maximum shifts ~400 cm^{-1} to lower energy.[12,33] The proposed explanation for the effect is that emission from state 1 is dipole forbidden but vibronically allowed to an excited vibrational level ($\hbar\omega = 400$ cm^{-1}) of the ground state. The fact that emission from the A_2 state is dipole forbidden in the idealized C_{2v} symmetry is consistent with this experimental observation.

Discussion

The localized model developed here successfully accounts for the following features of the MLCT excited states of $Ru(bpy)_3^{2+}$ and $Os(bpy)_3^{2+}$: (1) There are four low-lying MLCT states, the three lowest of which are close together energetically and the fourth is several hundred cm^{-1} higher in energy. (2) Emission from the lowest state (A_2) is dipole forbidden. (3) The limited polarization data for $Ru(bpy)_3^{2+}$ can be accounted for and leads to an explicit state assignment. Clearly more polarization data, particularly for $Os(bpy)_3^{2+}$, are needed to test the validity of the present model. The salient points here are as follows: (1) The localized model predicts that no more than four nondegenerate, low-lying excited states are present. (2) The four states have distinct spectroscopic characteristics. By contrast, for the delocalized case there could be five low-lying excited states, three of which have E symmetry.[5] The predictions for the delocalized case also originate from a parametric model. Since at this stage only four states have been observed, it should be straightforward to disprove the localized model if it were not appropriate. However, with the limited data available and no strong evidence to the contrary (vide infra), we conclude that the excited states are localized at all temperatures studied. At the very least, the model described here is directly relevant to fluid solutions, where previous evidence for localized excited states including resonance Raman spectra[14] and the solvent dependence of MLCT band energies[15] has been obtained.

Given the apparent successes of a localized model, it is necessary to consider recent experimental evidence that was cited as being consistent with delocalized excited states.[12] One observation was that emission from $Ru(bpy)_3^{2+}$ carried appreciable magnetic circular polarization (MCP), which was suggested to be inconsistent with a localized excited state since a localized excited state should have only linearly polarized emission. However, it is well-known that linearly polarized absorption and emission processes usually do carry magnetic circular polarization and that the magnitude can be quite appreciable.[34] A second observation was that the MCP of

(30) Kober, E. M.; Meyer, T. J., submitted for publication.
(31) (a) Caspar, J. V.; Meyer, T. J. *J. Am. Chem. Soc.* **1983**, *105*, 5583–5590. (b) Caspar, J. V.; Meyer, T. J. *Inorg. Chem.* **1983**, *22*, 2244–53. (c) Allen, G. H.; White, R. P.; Rillema, D. P.; Meyer, T. J. *J. Am. Chem. Soc.* **1984**, *106*, 2613–20.
(32) Yersin, H.; Gallhuber, E.; Vogler, A.; Kunkely, H. *J. Am. Chem. Soc.* **1983**, *105*, 4155–6.
(33) Baker, D. C.; Crosby, G. A. *Chem. Phys.* **1974**, *4*, 428–33.

the luminescence at 2 K changes signs as a function of the emission energy. Such a result implies that either the ground or excited state must be degenerate provided the emission comes from a single state.[34] However, the superposition of two emissions that carry opposite signs of MCP could also cause such a result. There are two possible ways in which this could occur: (1) Sufficient emission intensity exists from the two lowest states at 2 K. (2) Since the emission from the lowest state is dipole forbidden, there could be two (or more) vibronically allowed emissions from this state. In light of the other evidence favoring the localized alternative, it is difficult to accept the MCP luminescence data as proof of a delocalized excited state.

With regard to the predictions of the polarization ratios in Table IV, the following should be noted: (1) It is assumed that the X' and Y' directions are equivalent as required by D_3 symmetry. (2) It is assumed that the bpy ligand to which the electron is promoted is independent of whether the exciting light is X',Y' polarized. Under these circumstances, the value of $P(X',Y')$ should not exceed 0.14. However, as has been frequently noted, the value of $P(X',Y')$ for $Ru(bpy)_3^{2+}$ is higher than this ($\sim$0.2) in certain spectral regions.[4,16a,b,28a]

An explanation for $P > 0.14$ based on the localized model can be developed[16a] if assumptions 1 and 2 above are incorrect. From a straightforward coupling of linear oscillators, it can be seen from Figure 6 that Y'-polarized light should place the excited electron on bpy ligand $\sim$p with a probability of $^2/_3$ and on bpy ligands q or r each with a probability of $^1/_6$. X'-polarized light should place the excited electron on bpy ligands q or r each with a probability of $^1/_2$. For X'-polarized light the probability of the electron resulting on bpy ligand p is 0. Provided that the electron "hopping" rate between the bpy ligands is slow or comparable to the rate of excited-state decay, it is necessary to distinguish between the X' and Y' directions, and this could account for the regions of anomalous P values.

However, the gross behavior observed for the magnitude of P is accountable if assumptions 1 and 2 are valid and we have restricted our predictions to this regime. More sophisticated treatments, such as that of Carlin and DeArmond,[16a] which also take into account the electron "hopping" rate, may be necessary to explain the fine details of the observed variations in P. The subtle differences in polarization behavior observed between the Os and Ru complexes may also be resolvable in the same manner.

A more definitive experiment would involve the measurement of Z'-, Y'-, and X'-polarized emission from single-crystal samples as a function of temperature. The single-crystal experiment would provide clear evidence for both the number of excited states and their polarization properties.

As suggested above, a question naturally arises as to how the electron "hopping" rate between bpy ligands affects excited-state properties. For the reduced complex $[Fe(bpy)_2(bpy^{-}\cdot)]^+$, a hopping rate constant of $k \approx 10^8$ s^{-1} has been measured by EPR techniques at ambient temperatures. The thermal activation barrier for the process is $\sim$900 cm^{-1}.[17] If electronic coupling between ligands is the same in the ligand-reduced, e.g., $(bpy)_2Ru^{II}(bpy^{-}\cdot)^+$, and MLCT excited states, $(bpy)_2Ru^{III}(bpy^{-}\cdot)^{2+*}$, the ligand to ligand hopping rates would be comparable. Excited-state decay rates under ambient conditions are of a similar magnitude, and since both types of processes are each temperature and medium dependent, the interplay and coupling between them could lead to some interesting excited-state effects. As mentioned above, such an interplay could affect the "equivalence" of the X' and Y' axes, which would be apparent from polarization measurements for both single-crystal and randomly oriented glass samples.

However, ligand to ligand electron transfer should not play a role in the temperature dependence of excited-state decay rates for the present molecules. Irregardless of which bpy ligand acts as the acceptor site for the promoted electron, the resulting manifold of excited states, their relative energies and their respective decay rates should be identical. Since hopping from one bpy ligand to another cannot change these properties, it does not matter how fast or how slow this rate is and it cannot be measured by examining such properties as long as thermal equilibrium is maintained. The same situation exists for bis(bipyridine) complexes that have C_2 symmetry.

For bis(bipyridine) complexes with C_1 symmetry, e.g., $Ru(bpy)_2(CO)Cl^+$, the bpy ligands are no longer equivalent and there will be an energetic preference for the promoted electron to be localized on one of the bpy ligands. If the electronic environments at the two bpy ligands are sufficiently different, the two different types of $Ru^{III}(bpy^{-}\cdot)$ excited states could well give rise to manifolds of states that are quite different with respect to relative decay rates, relative energies, and probably state orderings as well. In such cases, the electron-hopping rate can play an important role and complicated excited-state behavior can result. A similar situation would result for mixed-chelate complexes such as $Ru(bpy)_2(phen)^{2+}$, and some data have been reported in this regard with mixed results.[35]

With the suggested assignment of the four lowest MLCT states as 1 = A_2, 2 = B_2, 3 = A_1, and 4 = B_1, it is possible to consider in more detail the requisite values of F and G. As noted above, in a general sense the suggested ordering of states demands that $0 < F < G$, which was the case chosen for illustration in Figures 3 and 4. For the specific case appropriate for $Os(bpy)_3^{2+}$, where the B_2 state occurs at $\sim$15 cm^{-1} above A_2 and the A_1 state at $\sim$50 cm^{-1} above A_2, the values of F and G must be quite large ($\geq$4000 cm^{-1}). By the same token, the B_1 state being $\sim$600 cm^{-1} above the A_2 state requires that the values for F and G be in the same range, 1000–2000 cm^{-1}. The suggested dilemma is, of course, subject to the values selected for K and λ as well as dependent on the assumption that the values for K and λ are isotropic. Further types of configuration interaction have also been neglected. At present we can only conclude that F and G are probably in the vicinity of 3000 cm^{-1}.

The approximate values of F and G can be utilized to make quantitative estimates of the percent singlet character in the four lowest lying MLCT states. For the B_2 and A_1 states, the percent singlet character is $\sim$3% for Ru and $\sim$12% for Os (note Figure 5). For the B_1 state, a reasonable estimate is 40–60% singlet character for both metals. As noted above, the lowest lying state, which is A_2 for both metals, is predicted to have $\sim$0% singlet character to a first approximation. Consequently, the three lowest states are essentially "triplet" states for both metals although the fourth state (B_1) has a strongly mixed spin character. Nonetheless, it is important to realize that there is a significant singlet character in these low-lying MLCT states that can influence excited-state properties. An example is the observation of energy transfer from the MLCT states to the singlet excited states of organic dyes, which electronically has an important component that is spin allowed.[36]

(34) (a) Richardson, F. S.; Riehl, J. P. *Chem. Rev.* **1977**, *77*, 773–92. (b) Schatz, P. N.; McCaffery, A. J. *Q. Rev. Chem. Soc.* **1969**, *23*, 552–84 and references therein.

(35) (a) Halper, W.; DeArmond, M. K. *J. Lumin.* **1972**, *5*, 225–37. (b) Crosby, G. A.; Elfing, W. H., Jr. *J. Phys. Chem.* **1976**, *80*, 2206–11. (c) Elfring, W. H., Jr.; Crosby, G. A. *J. Am. Chem. Soc.* **1981**, *103*, 2683–7. (d) Baggott, J. E.; Gregory, G. K.; Pilling, M. J.; Anderson, S.; Seddon, K. R.; Turp, J. E. *J. Chem. Soc., Faraday Trans. 2* **1983**, *79*, 195–210.

(36) Mandal, K.; Pearson, T. D. L.; Krug, W. P.; Demas, J. N. *J. Am. Chem. Soc.* **1983**, *105*, 701–7.

In another study, the differences in k_r and k_{nr} between the three lowest MLCT states in related polypyridyl complexes of Os(II) and Ru(II) was accounted for quantitatively by assuming that the MLCT states for Os had approximately 3 times as much singlet character as for Ru.[30] That estimate is substantiated here for states 2 (B_2) and 3 (A_1), although the present model is too unsophisticated to deal with state 1 (A_2), which is treated as a pure triplet state. However, it seems likely that the mechanism by which this state acquires singlet character will also involve spin–orbit coupling and the factor of 3 difference may be maintained. In any case, it is a noteworthy conclusion of the model that state 4 (B_1) has approximately the same amount of singlet character for either Ru or Os. Unfortunately, since the lifetime of this state for Ru is not known, this point cannot be verified.

From the data in Tables V and VI, it would appear that the energy splittings between the three lowest states for Os and Ru are rather similar. However, the model developed here predicts that, for similar F and G values, the energy splittings for the Os case should be significantly larger (a factor of 2–3) than for Ru because of the greater spin–orbit coupling constant. The resolution of this dilemma comes from considering the data collected for a variety of metal tris(substituted bipyridine or phenanthroline) complexes. For the Ru complexes, the second and third states occur at 8.5–10.1 and 30.1–64.2 cm^{-1}, respectively, above the lowest state.[6] For Os complexes, the values are 16–42 and 52–173 cm^{-1}, respectively.[9] Thus, in general, the prediction of the model appears to be substantiated. As is noted in greater detail elsewhere,[30] the energy splittings and excited-state decay rates derived for the complexes $Os(bpy)_3^{2+}$ and $Os(phen)_3^{2+}$ seem to be somewhat out of line when compared with data for related complexes.

A corollary to the present work is that the model developed here should also be appropriate to the MLCT excited states of related mono- and bis(bipyridine) complexes. Particularly important is the conclusion that no more than four low-lying MLCT states for second- or third-row transition-metal complexes should be important at ambient or lower temperatures except possibly for $M(bpy)_2LL'^{n+}$ complexes as noted above. In this regard it is interesting to note the report that the temperature-dependent excited-state properties of $Ru(bpy)_2(CN)_2$ and of some complexes of the type *cis*-$Ir^{III}(bpy)_2L_2$ require the presence of four states.[11] The values of F and G for any particular system must certainly depend upon the various ligands in such complexes, and consequently, different energy spacings and possibly even different state orderings could result. However, other than changes in the amount of singlet character present in each state, fundamental excited-state properties such as the polarization of the emission and the relative ordering of lifetimes of the various states will be unchanged.

It has recently been shown that room-temperature lifetimes for a variety of polypyridyl complexes of Os and Re depend upon the excited-state energy in an exponential manner[29,37] in quantitative agreement with the "energy gap law".[38] Similar results have been obtained for the MLCT excited-state lifetimes of Ru–bpy complexes at lower temperatures.[31] From Table V it can be seen that the lifetimes of the four low-lying MLCT states of $Os(bpy)_3^{2+}$ differ by more than 3 orders of magnitude and similar variations are expected to exist for the other complexes in the series alluded to above. As a consequence, the apparent agreement with the "energy gap law" seems to imply that the state of common symmetry (presumably B_1) is dominating excited-state properties at room temperature, which is the temperature of the experiment. However, careful temperature dependence studies are required to test this point and they are required to test the "energy gap" correlation quantitatively.

In order to explain the polarization properties, band structure, and circular dichroism for the complexes $M(bpy)_3^{2+}$, it is necessary to turn to a delocalized model.[4,5,39] However, the use of a delocalized model to account for such properties does not require that in the initially populated excited state the promoted electron is delocalized over all three bpy ligands. In fact, it has been shown that, at room temperature, the electronic polarization of the solvent medium can sense the instantaneous formation of the dipolar localized excited state $(bpy)_2M^{III}(bpy^{-}\cdot)^{2+}$.[15] The necessity for using a delocalized model to account for certain properties arises because of Coulombic coupling of the individual, localized transition moments as described by exciton theory.[39,40] This phenomenon is well-known and can lead to intramolecular coupling of localized transition moments, as in the present case, or to intermolecular coupling between different sites, as in crystals for example. The necessity of using a delocalized model for absorption spectra is a consequence of the fundamental nature of the light absorption act and holds no implication for the localized or delocalized nature of the excited state.

The ultimate question then becomes "What provides the basis for localization in the excited state?" This question provides one of the central issues in mixed-valence chemistry,[41] and in a real sense, the excited states of interest here are examples of mixed-valence systems. In mixed-valence compounds the question of localization vs. delocalization has been discussed in detail.[42] It has been concluded that the key factors are the relative magnitudes of the vibrational trapping energy for the exchanging electron arising from intramolecular and solvent vibrations compared to the delocalization energy arising from electronic coupling. Intramolecular vibrational trapping occurs for normal modes for which there are changes in the equilibrium displacement coordinate or frequency in the excited state. Trapping by the solvent occurs by charge-dipole interactions, whose magnitude depends upon $(1/D_{op} - 1/D_s)$, where D_{op} and D_s are the optical and static dielectric constants of the solvent. For polar solvents, $D_{op} < D_s$ and the trapping energy depends largely on the index of refraction n, since $D_{op} = n^2$. An alternate but equivalent criterion for localization is that vibrational trapping must provide a sufficiently strong vibronic (Jahn–Teller) splitting of the delocalized state for localization to occur.

For a thermally equilibrated excited state like $Ru(bpy)_3^{2+*}$, the shifts in equilibrium normal coordinates between the excited and ground state lead to significant intramolecular and solvent trapping on the basis of the analysis of low-temperature emission profiles.[29,31,37,43] In the emission process, $(bpy)_2Ru^{III}(bpy^{-}\cdot)^{2+*} \rightarrow (bpy)_2Ru^{II}(bpy)^{2+}$, an electron transfer occurs involving the bound $bpy^{-/0}$ couple. In that sense emission is analogous to electron transfer between ligands in the excited state, $(bpy)_2Ru^{III}(bpy^{-}\cdot)^{2+*} \rightarrow (bpy)(bpy^{-}\cdot)Ru^{III}(bpy)^{2+*}$. From emission spectral fitting, vibrational

(37) (a) Caspar, J. V.; Sullivan, B. P.; Kober, E. M.; Meyer, T. J. *Chem. Phys. Lett.* **1982**, *91*, 91–5. (b) Caspar, J. V.; Meyer, T. J. *J. Phys. Chem.* **1983**, *87*, 952–7.

(38) (a) Freed, K. F.; Jortner, J. *J. Chem. Phys.* **1970**, *52*, 6272–91. (b) Lin, S. H.; Bersohn, R. *Ibid.* **1968**, *48*, 2732–6. (c) Lin, S. H. *Ibid.* **1966**, *44*, 3759–67. (d) Englman, R.; Jortner, J. *Mol. Phys.* **1970**, *18*, 145–64.

(39) McCaffery, A. J.; Mason, S. F.; Norman, B. J. *J. Chem. Soc. A* **1969**, 1428–41.

(40) (a) Davydov, A. S. "Theory of Molecular Excitons"; McGraw-Hill: New York, 1962. (b) Craig, D. P.; Walmsley, S. H. "Excitons in Molecular Crystals"; W. A. Benjamin: New York, 1968.

(41) Brown, D. B., Ed. "Mixed-Valence Compounds", D. Reidel: Boston, 1980.

(42) (a) Wong, K. Y.; Schatz, P. N. *Prog. Inorg. Chem.* **1981**, *28*, 369–449. (b) Cribb, P. H.; Nordholm, S.; Hush, N. S. *Chem. Phys.* **1979**, *44*, 315. (c) Schatz, P. N. In ref 41. (d) Hush, N. S. In ref 41.

(43) (a) Caspar, J. V.; Westmoreland, T. D.; Allen, G. H.; Bradley, D. G.; Meyer, T. J.; Woodruff, W. H. *J. Am. Chem. Soc.* **1984**, *106*, 3492–500. (b) Kober, E. M.; Meyer, T. J. *Inorg. Chem.*, in press.

trapping inhibiting bpy–bpy electron transfer occurs by medium-frequency, bpy-based vibrations with $2\chi_M \simeq 2700$ cm^{-1}, low-frequency, apparently Ru–N based modes with $2\chi_L \simeq 1000$ cm^{-1}, and solvent modes with $2\chi_S \approx 1000$ cm^{-1}.[15,43] The χ values are 4 times the classical vibrational trapping energies, and the factor of 2 includes contributions from both ligands for the bpy–bpy electron-exchange process. It is interesting to note that using these values gives a classical energy of activation of $E_a \approx 1200$ cm^{-1}, which is near the experimental value of $\sim$900 cm^{-1} found for bpy–bpy electron transfer in $Fe(bpy)_2(bpy^{-\cdot})^+$.[17] Given the evidence for vibrational trapping, if electronic coupling between ligands is sufficiently small, localization is expected to occur.

However, the situation with regard to the solvent dependence of absorption bands is quite different.[15] Here the optical excitation ($\sim 10^{15}$ s) is short on the time scales for equilibration of the intramolecular modes and of the low-frequency solvent polarization modes. As a consequence, in the excited state, the intramolecular and low-frequency solvent orientational modes at each ligand are those appropriate for the symmetrical ground state. Only the electronic polarization of the solvent medium (D_{op}) can respond to the excitation process. Because this instantaneously follows the electron distribution of the solute, it would not seem to provide a barrier to the bpy–bpy electron-exchange process. However, it does favor a localized excited state over a delocalized one because of the added dipole solvation energy. The variation of absorption band energies with D_{op} establishes this quite clearly.[15]

The observation of excitation localized to a single ligand remains a reasonable observation even in the absence of significant vibrational trapping as long as electronic coupling between the ligands is small. In the absence of any trapping, the frequency of the redistribution of the exchanging electron from one ligand to another is given by $\nu_{et} \approx 4V/h$, where V is the delocalization or resonance energy,[44] and statistical effects are not included. Even with $V = 800$ cm^{-1} (0.1 V), ν_{et} is still $\sim 10^{14}$ s^{-1} and electron hopping between ligands would be too slow to couple significantly with the optical excitation. Actually, it is interesting to note that if V were of the magnitude mentioned above, the excited state could be "delocalized" for a short time period following excitation but before the processes leading to vibrational equilibration occur.

It might be argued that the situation is different in a glass or in the solid state, where orientational correlation times for the surrounding trapping dipoles of the medium are restricted and may be long on the time scale for excited-state decay. However, even in the absence of medium trapping, vibrational trapping by intramolecular vibrational modes does exist. The time scale for an individual molecular emission event is rapid on the vibrational time scale. As is the case for light absorption, even in the absence of vibrational trapping, relatively strong electronic coupling between bpy ligands would be required for interligand electron hopping to become competitive with the emission process.

Acknowledgments are made to the Department of Energy under Grant no. DAAG29-79-K-0111 for support of this research and to the Morehead Foundation for generous fellowship support of E.M.K. We also wish to thank Dr. H. Yersin for a copy of ref 32 in advance of publication.

Registry No. $Ru(bpy)_3^{2+}$, 15158-62-0; $Os(bpy)_3^{2+}$, 23648-06-8.

(44) Duke, C. B. In "Tunneling in Biological Systems"; Chance, B., et al., Eds.; Academic Press: New York, 1979; pp 31–65.

Contribution from the Department of Chemistry, Indian Institute of Technology, Madras 600 036, India

EPR, Magnetic, and Structural Investigations on the Weak-Exchange Heisenberg Linear Chain Bis(*N*-methylphenazinium) Bis(dicyanoethenedithiolato)cuprate(II), $[(NMP)_2][Cu(mnt)_2]$

P. KUPPUSAMY, B. L. RAMAKRISHNA, and P. T. MANOHARAN*

Received November 22, 1983

The title compound $[(NMP)_2][Cu(mnt)_2]$ crystallizes in the monoclinic space group $P2_1/n$ with $a = 11.417$ (2) Å, $b = 8.126$ (2) Å, $c = 17.674$ (7) Å, $\beta = 92.11$ (2)°, and $Z = 2$. The structure, including H, was solved by Patterson and Fourier methods and refined by full-matrix least squares to $R = 0.048$, based on 1944 observations. The compound forms a kind of mixed stack with a donor–acceptor sequence DAD–DAD along the a axis. The static susceptibility measurements showed the exchange to be weak. Single-crystal EPR in the ac^* plane, where the two sites are magnetically equivalent, showed single exchange-narrowed Lorentzian lines with hyperfine dominated line width. The relative magnitudes of various Hamiltonians are $\mathcal{H}_{Zee} > \mathcal{H}_{ex} > \mathcal{H}_{hyp} > \mathcal{H}_{dip}$. The angular dependence of the line width in the ac^* plane along with the computed second moments was used to evaluate the high-temperature Fourier components of the autocorrelation function $C(t)$ and $C^2(t)$. The computed nonsecular components were shown to follow from either the Blume–Hubbard model with $\hat{J} = 2100$ G or from the Anderson–Weiss model with $J = 1175$ G.

Introduction

The metal dithiolate complexes $[M(S_2C_2R_2)_2]^{n-}$ where R = CN, CF_3, etc., are a class of interesting compounds that exhibit low-dimensional cooperative phenomena[1,2] associated with their columnar crystallographic packing. Certain d^7 complexes with M = Ni, Pd, or Pt and R = CN exhibit quite strong apparently one-dimensional exchange coupling with J_o of the order of 10^2 cm^{-1} for dimeric stacks[3] and of the order of unity for regular stacks.[4] On the other hand, the Cu(II) analogue, $[Cu(mnt)_2]^{2-}$ shows quite varied behavior in the small J_o regime. For example, $[(NEt_4)_2][Cu(mnt)_2]$ with J_o

(1) Keller, H. J., Ed. "Low Dimensional Cooperative Phenomena"; Plenum Press: New York, 1975.
(2) Interrante, L. V., Ed. "Extended Interactions between Metal Ions in Transition Metal Complexes"; American Chemical Society: Washington, DC, 1974; ACS Symp. Ser. No. 5.
(3) Weiher, J. F.; Melby, L. R.; Benson, R. E. *J. Am. Chem. Soc.* **1964**, *86*, 4329.
(4) Manoharan, P. T.; Noordik, J. H.; de Boer, E.; Keijzers, C. P. *J. Chem. Phys.* **1981**, *74*, 1980.

0020-1669/84/1323-3886$01.50/0